

Efficient plasmonic nanostructures for thin film solar cells

Valeria Marrocco^a, Marco Grande^a, Maria Antonietta Vincenti^b, Giovanna Calò^a, Vincenzo Petruzzelli^a and Antonella D'Orazio^a

^a Dipartimento di Elettrotecnica ed Elettronica, Politecnico di Bari, Via Re David 200, 70125 Bari, Italy

^b AEGIS Technologies Group, 410 Jan Davis Dr., Huntsville, AL, USA, 35806

ABSTRACT

Recent scientific publications have highlighted the possibility of enhancing solar conversion efficiency in thin film solar cells using surface plasmon (SP) waves and resonances. One main strategy is to deposit layers of metal nanoparticles on the top of a thin film silicon solar cell which can increase light absorption and consequently the energy conversion in the frequency range where the silicon intrinsic absorptance is low. In this paper, we investigate the effects produced on the light absorption and scattering by silver nanoparticles, arranged in a periodic pattern, placed on the top of amorphous silicon (α -Si) thin layer. We propose different geometry of metal objects, quantifying the scattering (back and forward) determined by the nanoparticles in dependence of their shapes and Si thickness. The analysis reveals that the thickness of the substrate has huge influence on the scattering, in particular on the back one, when the nanoparticles have corners, whereas it seems less dramatic when rounded profiles are considered (nanospheres).

Keywords: metal nanoparticles, plasmon resonance, scattering, field enhancement, thin film.

1. INTRODUCTION

Electric energy production has been revolutionised by the use of renewable and sustainable energy sources; especially in the last twenty years photovoltaics has been playing the major role, due to the mature silicon-based technology to produce the photovoltaic modules composed by the elementary components connected in a more complex grid: the solar cells. Solar cell market is based mostly on crystalline silicon wafers, having thickness ranging between 200-300 μm . Since the most of solar module cost is ascribed to the cost of the silicon wafers, the need of an alternative and less expensive technology becomes almost mandatory for both scientific and commercial community.

Thin film solar cells seem to be the best alternative to the well-established monocrystalline wafer technology, since thin film solar cell utilises cheap substrates, such as plastic, glass or stainless steel, where a variety of semiconductors (cadmium telluride (CdTe), copper indium diselenide (CIDS) as well as amorphous and poly and micro-crystalline silicon) having thickness ranging from 0.3 up to 2 μm , can be grown upon them. Since the thicknesses the thin film technology deal with are very small, one can expect less capability of the semiconductor material to trap the light insight, because of reasonable small values of absorptance. Then, at first glance, thin film technology could be seen as a less efficient way to convey light to a significant photocurrent production. This issue has driven and stimulated the research activity to find new strategies aimed to efficient light trapping and concentration mechanisms.

In the last decade surface plasmon (SP) resonance [1] has been employed to enhance light absorption in thin film solar cells, thanks to the scattering caused by noble metal nanoparticles or islands deposited on the semiconductor surface. The introduction of noble metal nanoparticles into or on solar cells is able to induce a significant increase of the photocurrent indeed, since two main phenomena can take place nearby those objects: light scattering and near-field concentration of light. Both mechanisms are present in this scenario, but the preponderance of one with respect to the other is strictly dependent on the nanoparticle size and shape, semiconductor absorption and electrical design of solar cells [2-5]. As the metal nanoparticle size is increased one can generally expect [3-5] a red shift along with a broadening of the plasmon resonance: this can in principle affect the scattering positively, as for solar cell applications a broad band light trapping is strongly recommended. A trade off is yet required because increasing the nanoparticle size leads to an overall reduction of the scattering cross section [4-5]. To date, noble metal nanoparticles have been used to increase the photocurrent for

different type of thin film solar cells: heterojunction with amorphous silicon [6], CdTe- based, organic solar cells [7-10]. In reference [11], a different approach is used by the authors: in fact sub-wavelength scatterers are considered to couple sunlight into guided modes in thin film Si and GaAs plasmonic solar cells whose back interface is coated with a corrugated metal film. Therefore, SPs seem to offer a great chance to modify without twisting the pre-existing solar cell technology dramatically, providing also the possibility of tailoring the SP dispersion and hence tuning the SP resonance at wanted wavelengths [6,11-13] by operating a proper choice of the materials, metals and semiconductors [14-15].

In addition to the aforementioned solutions, the so-called nanoantennas [16-18] promise to accomplish similar goals in photovoltaics. This fact is not surprising considering that an elementary nanoantenna exploits noble metal (gold or silver) nanoparticles, mounted on a glass or silica substrate, and is able to localise and emit light in the near field, when a plane wave at a certain frequency impinges on the structure. Therefore, they behave more like optical concentrators enabling high local field intensity rather than scattering objects. Optical antennas are not new in the optical field, as they are already employed in different applications and technologies, such as spectroscopy (NSOM) [17-18], enhanced Raman scattering [21-22], optical nanolithography [23], among others. When two single nanoparticles are separated by a well defined distance (gap), an intense localization of the electromagnetic field in the sub-wavelength gap can be observed. The dramatic ability in localising and transmitting the input field [24-31] in such small apertures in the visible and infrared regimes has its basis on the enhanced transmission phenomenon [26]. The choice of a specific shape for a nanoantenna is strictly dependent on the further application: for instance, bow-tie and spirals are more suitable for wider band operation, though the enhancement of the localized field is less intense than the one shown by nanorods. Also linear arrays of noble metal nanoparticles (elliptical dimers and rounded corners nanorods) have been studied both numerically and experimentally [32-35].

Light absorption, forward and back-scattering and near-field coupling and enhancement produced by noble metal nanoparticles have been thus widely explored; loss mechanisms, such as back-scattering, have been analyzed and discussed to obtain optimized parameter designs, determining, for instance, the appropriate distance among nanoparticles and sizes. However, to the best of our knowledge, the relation between noble nanoparticle shape and substrate thickness has not been yet thoroughly investigated in terms of scattering and light concentration. For this reason, the issue this paper is focused on concerns the numerical analysis and the evaluation of the effects induced on back and forward scattering by structures comprising metal nanoparticles, having different shapes, located on finite substrates. We will show in details how the Si substrate having finite thickness, considered as a resonant cavity, origins resonant modes which deeply affect the back and forward scattering behavior of metal nanoparticles in different ways, depending on their shapes.

2. NUMERICAL ANALYSIS

Arrays of Ag nanoparticles, cubic nanobricks and nanospheres, placed on infinite and finite Si substrates have been considered: the study has been performed using a proprietary code based on FDTD including Drude model used to fit the experimental data of the complex dielectric permittivity of silver [36]. Figure 1 provides the sketch of the analyzed structures, along with the excitation scheme and the field monitors used in our FDTD calculations. On the left, an array of cubic nanobricks, having the side equal to $s=40$ nm, are spaced each other of a variable distance (period) and located on silicon substrate ($n = 3.45$). On the right, the same structure comprises an array of Ag nanospheres having diameter equal to $D=40$ nm. The field recording surfaces and the excitation scheme used in the FDTD calculation are also depicted. The incident field is a plane wave having a Gaussian temporal behavior, tuned between 350 nm and 750 nm; in all the calculations, the excitation surface is placed 150 nm above the silver nanoparticles. The back-scattering surface is located 20 nm behind the excitation plane and the forward scattering surface is placed in the middle of the Si substrate. The analyses are carried out comparing two main cases: array of Ag nanobricks and nanospheres on semi-infinite lossless Si substrate and on a 100 nm thick lossless Si substrate. Moreover, we have evaluated how the scattering is influenced by the number of nanoparticles and their size. To complete our study, we have investigated also how the scattering is modified when the Si thickness is equal to 300 nm, 500 nm and 1000 nm.

Forward and back-scattering, for all analyses, are evaluated considering the Poynting vector recorded at the indicated scattering surfaces in presence of nanoparticles normalized to the Poynting vector calculated in absence of nanoparticles. The choice of such thin layers of Si relies on the will to emphasize the effect of substrate thickness on forward and backward scattering induced by metal nanoparticles, neglecting the losses ascribed to the dielectric material.

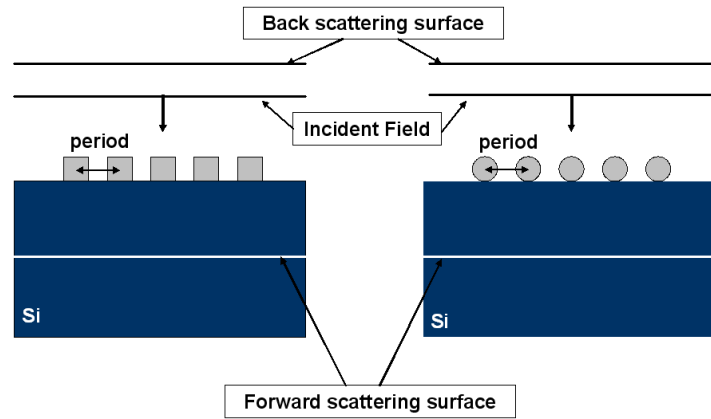


Figure 1: Sketch of the analyzed structures and FDTD-excitation and field monitor schemes.

2.1 Silver nanoparticles on semi-infinite Si substrate

When nanoparticles are placed on semi-infinite substrate, the behaviour of forward and back-scattering depends only on their size and the distance between them. Figure 2 reports the behaviour of both scatterings when five nanobricks at different spacing (period) are considered; an enhanced forward scattering is accomplished around 520 nm for period ranging from 60 nm up to 100 nm. For period equal to 150 nm and 200 nm the peak is shifted around 630 nm: in these cases the presence of nanoparticles does not affect part of the range of the visible spectrum (up to 500 nm), where no enhanced forward scattering can be observed.

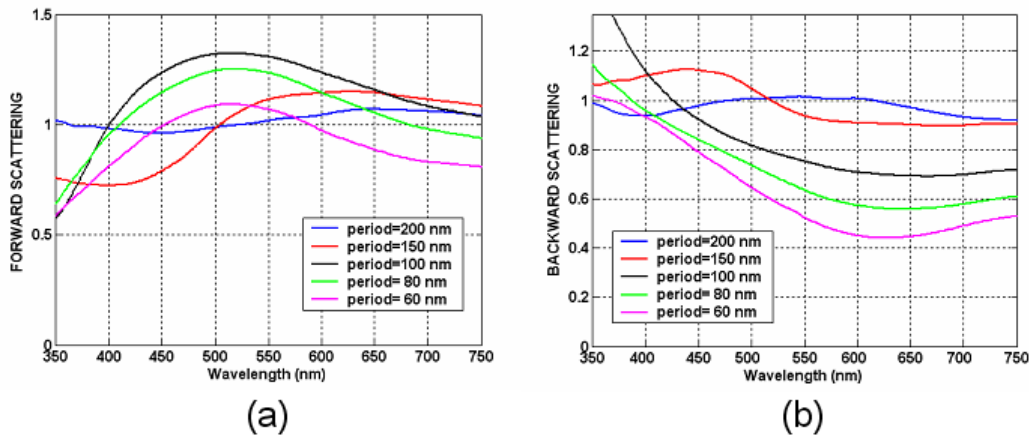


Figure 2: Forward (a) and back (b) scattering for an array of five nanobricks placed on semi-infinite Si substrate as the period is varied.

The reason relies on the fact that the metal nanobricks are far enough from each other and no significant light interaction among the nanoparticles at lower wavelengths can be efficiently accomplished, as can be clearly noticed by the electric field enhancement shown in Figure 3.

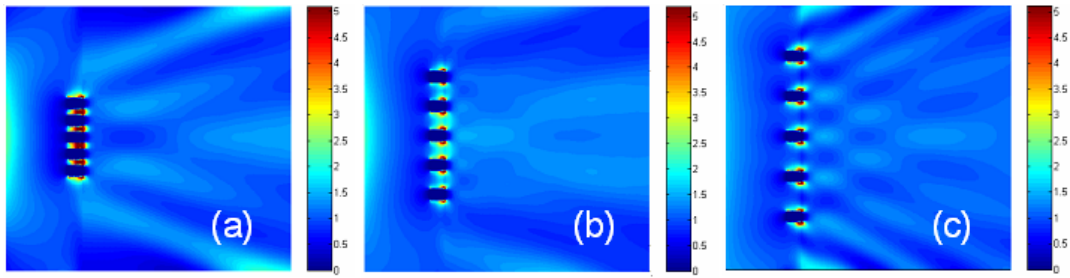


Figure 3: Electric field enhancement at $\lambda = 520$ nm when the period of the nanobricks array is equal to (a) 60 nm, (b) 100 nm and (c) 150 nm.

When one deals with nanospheres (Figure 4a) the forward scattering has similar behavior as the period is progressively varied, though the maximum value of the peak recorded in this case is lower than the co-respective curve calculated for the nanobricks. Figure 4b depicts the back scattering: the behavior is definitely different from the previous case, as all plots display a minimum around 340 nm and the maximum values are kept below unity for the whole wavelength range. This fact suggests that the back scattering is less intense than the one shows by the silicon without particles, since the Ag nanospheres are able to trap and concentrate light efficiently among them (Figure 5).

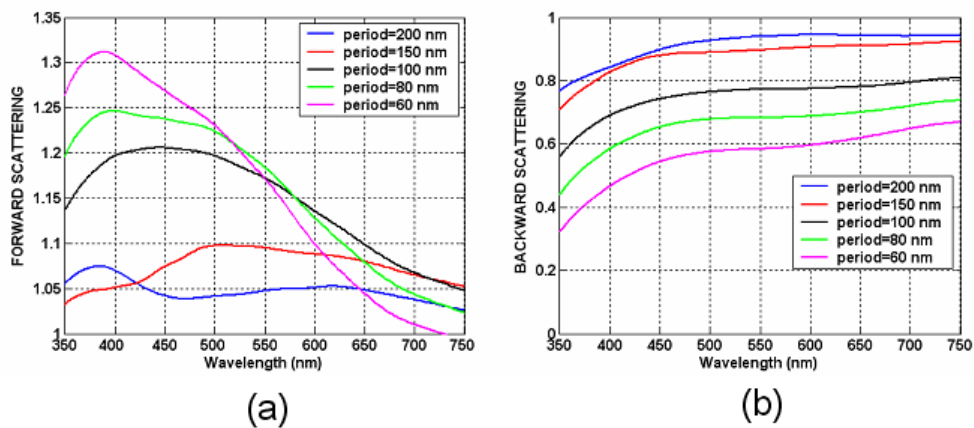


Figure 4: Forward (a) and back (b) scattering for an array of five nanospheres placed on semi-infinite Si substrate as the period is varied.

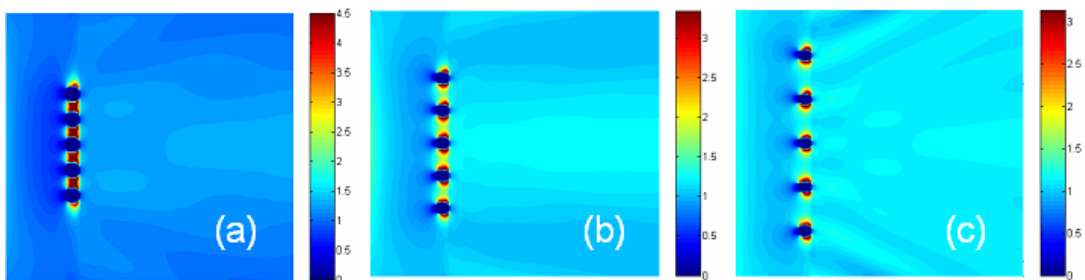


Figure 5: Electric field enhancement at $\lambda = 480$ nm when the period of the nanobricks array is equal to (a) 60 nm, (b) 100 nm and (c) 150 nm.

2.2 Silver nanoparticles on Si substrate of finite thickness

The situation is completely different when a finite substrate is considered. The enhanced peaks of the nanobricks array are blue-shifted, since the effective refractive index of the overall structure is reduced, but the intensities are considerably higher (almost doubled) and the forward scattering band is reasonably reduced (almost halved), as well (Figure 6).

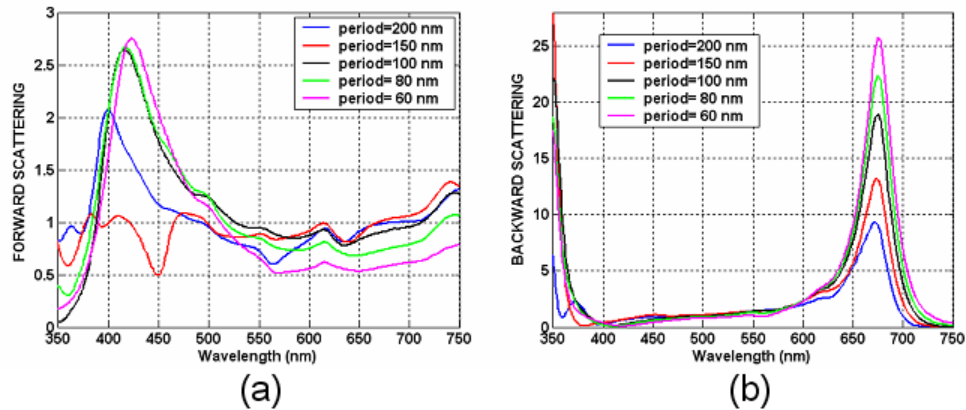


Figure 6 : Forward (a) and back (b) scattering for an array of five nanobricks placed on 100 nm thick substrate as the period is varied.

Nevertheless, the behavior of the forward scattering for a period equal to 150 nm is dramatically changed: in fact, together with the expected oscillating behavior, in correspondence of a wavelength equal to 450 nm, where structures with different period display the maxima in the forward scattering, the red curve displays a minimum having intensity equal to 0.5. Also an important variation in the back-scattering in dependence on the finite nature of the substrate can be noted. Nanobricks on semi-infinite substrate displays a back-scattering behavior (Figure 2b) which is somehow complementary to the forward scattering (Figure 2a), but when the finite substrate is considered two main peaks for each curve, around $347 < \lambda < 365$ nm and $668 < \lambda < 690$ nm, respectively, appear (Figure 6b). The nature of these peaks can be ascribed to the resonant modes rising in the finite dielectric (the spectral position shift is determined by different effective refractive index value in the structure as the nanoparticle period is varied). One can note the huge value of the back-scattering: it is worth stressing that such high intensities have sense if one keeps in mind that the back-scattering comprising metal nanoparticles is normalized to that produced by the only finite dielectric with no scattering objects onto it. In order to evaluate all possible changes induced on the scattering behavior by the variation of the physical parameters, further analyses have been carried out varying the number in the array of nanoparticles and their size, keeping the period and the thickness of the silicon substrate equal to 100 nm (Figure 7), respectively.

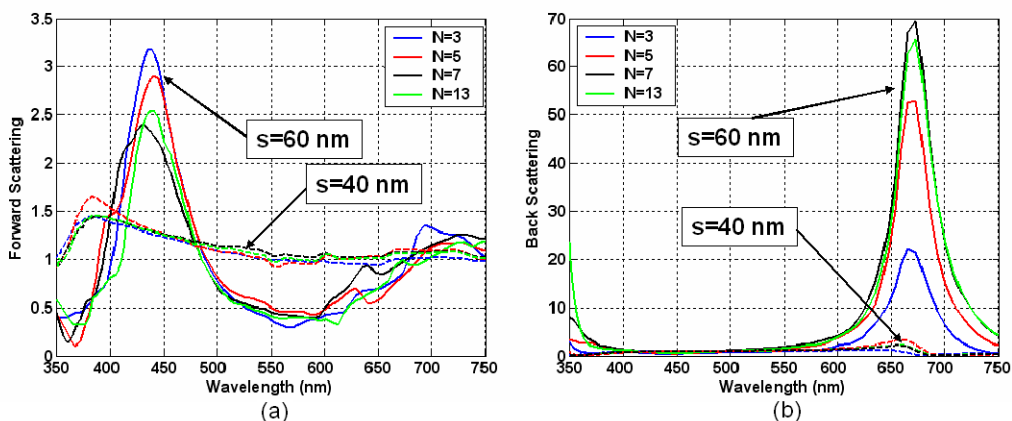


Figure 7: Forward (a) and back (b) scattering for array of nanobricks as the number of nanoparticles N is varied: the side is varied from $s=40$ nm to $s=60$ nm; the period is kept equal to 100 nm and the Si thickness is equal to 100 nm.

When the number of nanobricks is increased, one can expect an improvement in the performance: by the inspection of the dashed lines in Figure 7, it is clear that the forward scattering is not subjected to the supposed enhancement, whilst the back scattering is increased in correspondence of the resonant mode due to the finite substrate. An increase in the number of the metal nanoparticles leads to an increase of metal quantity on the silicon surface, so the enhancement in the forward scattering and light localization between the nanoparticles is compensated by the increase of metal losses and back scattering. If the size of the nanobricks is varied from 40 nm to 60 nm (solid lines in Figure 7), the cross section of the nanoparticles is varied, thus an effective enhancement in both forward and back scattering can be appreciated. But also in this case, it is evident that when the number of the nanoparticles increase, the forward scattering does not follow an intuitive behavior; as already observed for the previous case, the losses ascribed to the metal and back scattering play their role invalidating the supposed forward scattering improvement. The increase in the nanobricket size also involves a change in the maximum peak (red-shift as expected) and a shrink in the enhanced forward scattering band. Moreover, in correspondence of the end of the visible spectrum the peak due to the finite substrate is even more boosted, reaching an amazing value of 70. When one deals with nanospheres, anyway, the influence of substrate thickness seems less dramatic. Comparing Figure 8a and 4a, a slight blue-shift in the peak positions and a higher intensity (~ 30%) can be observed in presence of finite substrate. The behavior of the forward scattering is very similar, though the forward scattering band is comprehensibly reduced in the case of finite substrate. In presence of finite substrate one resonant peak is quite evident in the plots of the back scattering (Figure 8b): in this case, conversely to the semi-infinite substrate study, the presence of the finite substrate suppresses the back scattering right in correspondence of the resonant mode wavelength. But this phenomenon is not observed in any case: also for the nanospheres we have studied the possible changes the scattering is subjected to when the number of nanoparticles and their size are varied, keeping the period and the thickness of the silicon substrate equal to 100 nm.

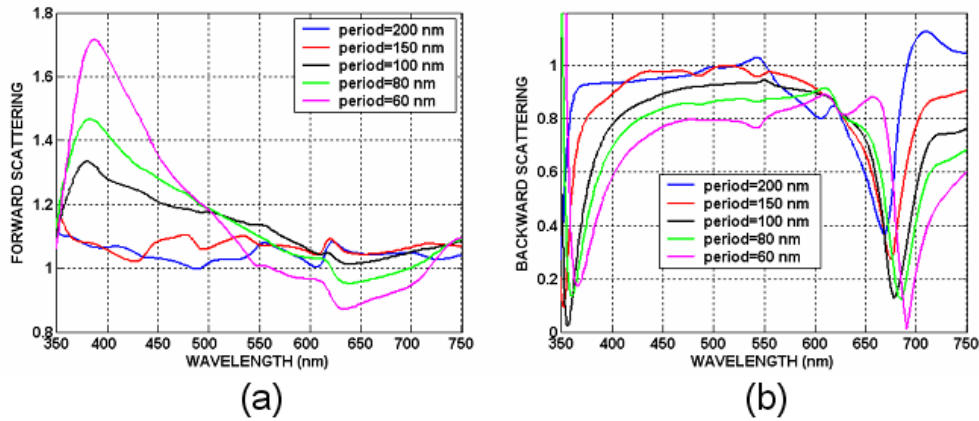


Figure 8: Forward (a) and back (b) scattering for an array of five nanospheres placed on 100 nm thick substrate as the period is varied.

By the inspection of the dashed lines in Figure 9, one can note that as the number of nanospheres is increased, the forward scattering does not experience the expected enhancement, whilst the back scattering is boosted and not reduced in correspondence of the resonant mode due to the finite substrate. If the diameter of the nanospheres is varied from 40 nm to 60 nm (solid lines in Figure 9), the cross section of the nanoparticles is decreased and an effective enhancement in both forward and back scattering can be appreciated, once again. The increase of the nanosphere size induces a red-shift in the maximum peak and the enhanced forward scattering band is decreased (in the green region of the visible spectrum the forward scattering values are below unity) and, in correspondence of the end of the visible spectrum, the peak in the back scattering due to the finite substrate is boosted, reaching a value of 8.

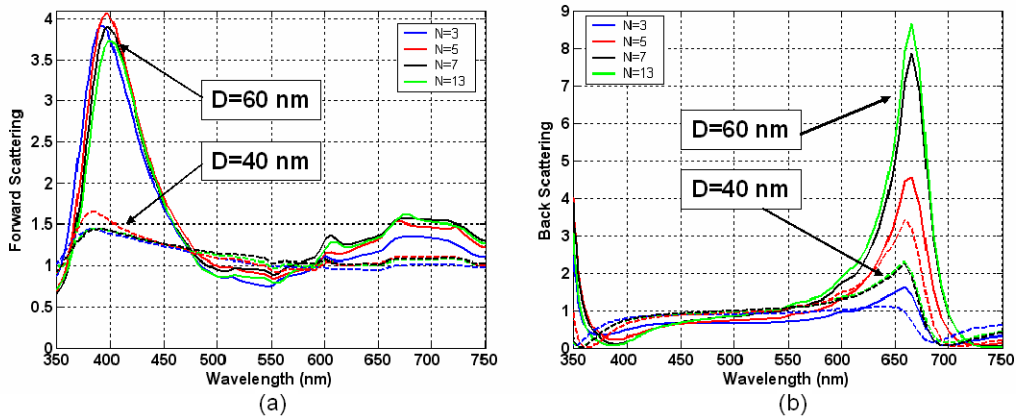


Figure 9: Forward (a) and back (b) scattering for array of nanospheres as the number of nanoparticles N is varied: the diameter is varied from $D=40$ nm to $D=60$ nm; the period is kept equal to 100 nm and the Si thickness is equal to 100 nm.

For sake of completeness, different substrate thicknesses (300 nm, 500 nm and 1000 nm) have been considered in order to confirm that the finite substrate, acting as a resonant cavity, can improve or worsen forward and back scattering in the visible range. The increase of the substrate thickness, in fact, induces the appearance of multiple resonant modes and Figure 10 and 11 witness this effect both in forward and backward scattering, evaluated for the array of nanobricks ($s=40$ nm) and nanospheres ($D=40$ nm), respectively, having period equal to 100 nm.

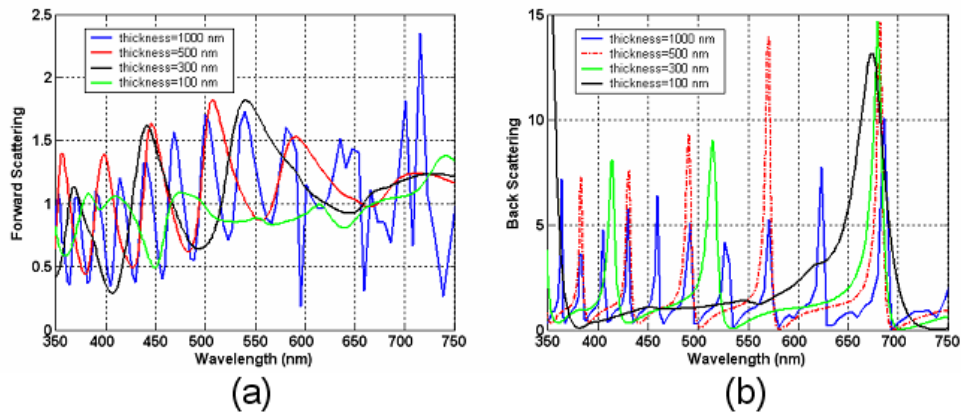


Figure 10: Forward (a) and back (b) scattering for an array of five nanobricks considering $s=40$ nm and period = 100 nm, as the substrate thickness is varied.

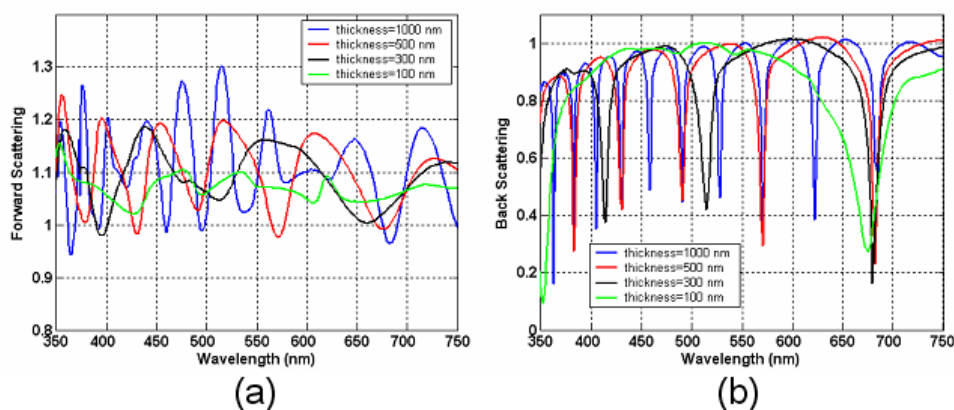


Figure 11: Forward (a) and back (b) scattering for an array of five nanospheres considering $D = 40$ nm and period = 100 nm, as the substrate thickness is varied.

3. CONCLUSION

In conclusion, when metal nanoparticles are chosen to improve the efficiency in thin film technology, we have shown that along with the size, shape and number of the nanoparticles, it is important to take care of the influence the finite substrate has on forward and back scattering. When nanobricks are considered the finite thickness of the substrate implies a huge increase in the forward scattering, enhancing the light transmission in the substrate, and in back-scattering, leading to the possibility of controlling the light extraction efficiency in correspondence of well determined wavelengths, i.e. resonances originating inside the finite dielectric. When nanospheres are considered, the forward scattering is less improved than that observed in the previous case, but the back-scattering can be significantly reduced in correspondence of the resonant peaks, though this effect can be observed for reduced size and number of nanoparticles. These results can lead to the design of optimized thin solar cells featuring enhanced transmission band matched to the solar spectrum peaks

REFERENCES

- [1] Raether, H. "Surface polaritons on smooth and rough surfaces and on gratings", Springer-Verlag Berlin (1988)
- [2] Catchpole, K.R. and Polman, A. "Plasmonic solar cells", *Optics Express* 16, 21793-21800 (2008).
- [3] Catchpole, K.R. and Polman, A. "Design principles for particle plasmon enhanced solar cells", *Appl. Phys. Lett.* 93,191113 (2008).
- [4] Kelly, K.L., Coronado, E., Zhao, L.L. and Schatz, G.C. "The optical properties of metal nanoparticles: the influence of size, shape and dielectric environment", *Journal of Physical Chemistry B* 107, 668-677 (2003).
- [5] Langhammer, C., Kasemo, B. and Zoric, I. "Absorption and scattering of light by Pt, Pd, Ag and Au nanodisks: absolute cross sections and branching ratios", *Journal of Chem. Phys.*, 126,194702 (2007).
- [6] Losurdo, M., Giangregorio, M. M., Bianco, G. V., Sacchetti, A., Capezzuto, P. and Bruno, G., "Enhanced absorption in Au nanoparticles/a-Si:H/c-Si heterojunction solar cells exploiting Au surface plasmon resonance", *Solar Energy Materials & Solar Cells*, 93, 1749-1754 (2009).
- [7] Pillai, S., Catchpole, K.R., Trupke, T., Green, M.A. "Surface plasmon enhanced silicon solar cells", *J. Appl. Phys.* 101, 093105.1–093105.8 (2007).
- [8] Schaadt, D.M., Feng, B., Yu, E.T. "Enhanced semiconductor optical absorption via surface plasmon excitation in metal nanoparticles", *Appl. Phys. Lett.* 86, 063106.1–063106.3 (2005).
- [9] Stenzel, O., Stendhal, A., Voigtsberger, K., von Borczyskowski, C. "Enhancement of the photovoltaic conversion efficiency of copper phthalocyanine thin film devices by incorporation of metal clusters", *Sol. Energy Mater. Sol. Cells* 37, 337–348 (1995).
- [10] Duche, D., Torchio, P., Escoubas, L., Monestier, F., Simon, J.J., Flory, F., Mathian, G. "Improving light absorption in organic solar cells by plasmonic contribution", *Solar Energy Materials & Solar Cells* 93, 1377-1382 (2009).

- [11] Ferry, V.E., Sweatlock, L. A., Pacifici, D. and Atwater, H. A. "Plasmonic Nanostructure Design for Efficient Light Coupling into Solar Cells", *Nano Lett.* 8, n.12, 4391-4397 (2008).
- [12] Martens, H., Verhoeven, J., Polman A. and Tichelaar, F.D. "Infrared surface plasmon in two-dimensional silver nanoparticles arrays in silicon", *Appl. Phys. Lett.* 85, 1317-1319 (2004).
- [13] Jung, Y. S., Wuenschell, J., Kim, H. K., Kaur, P. and Waldeck, D. H. "Blue-shift of surface plasmon resonance in a metal nanoslit array structure", *Optics Express* 17, 16081-16091 (2009).
- [14] Hägglund, C. and Kasemo, B. "Nanoparticle Plasmonics for 2D-Photovoltaics: Mechanisms, Optimization, and Limits", *Opt. Express* 17, 11944 -11957 (2009).
- [15] Centeno, A., Breeze, J., Ahmed, B., Reehal, H. and Alford, N. "Scattering of light into silicon by spherical and hemispherical silver nanoparticles", *Opt. Letters* 35, 76-79 (2010).
- [16] Muhlschlegel, P., Eisler, H.J., Martin, O.J.F., Hecht, B., Pohl, D.W. "Resonant optical antennas", *Science* 308 1607-1609 (2005).
- [17] Cubukcu, E., Kort, E. A., K., Crozier, B. and Capasso, F., "Plasmonic laser antennas", *Appl. Phys. Lett.* 89, 093120 (2006).
- [18] Yu, N., Cubukcu, E., Diehl, L., Belkin, M. A., Crozier, K. B., Capasso, F., Bour, D., Corzine, S. and Höfler, G. "Plasmonic quantum cascade laser antenna", *Appl. Phys. Lett.* 91, 173113 (2007).
- [19] Aizpurua, J., Bryant, G.W., Richter, L.J., Garcia de Abajo, F.J., "Optical properties of coupled metallic nanorods for field-enhanced spectroscopy", *Phys. Rev. B* 7, 1235420 (2005).
- [20] Farahani, J.N., Pohl, D.W., Eisler, H.-J., Hecht, B. "Single quantum dot coupled to a scanning optical antenna: a tunable superemitter", *Phys. Rev. Lett.* 95, 017402 (2005).
- [21] Poliakov, E.Y., Shalaev, V.M., Markel, V.A. and Botet, R. "Enhanced Raman scattering from self-affine thin films", *Opt. Lett.* 21, 1628-1630 (1996).
- [22] Fromm, D.P., Sundaramurthy, A., Kinkhabwala, A., Schuck, P.J., Kino, G.S., Moerner, W.E. "Exploring the chemical enhancement for surface-enhanced Raman scattering with Au bowtie nanoantennas", *J. Chem. Phys.* 124, 061101 (2006).
- [23] Sundaramurthy, A., Schuck, P.J., Conley, N.R., Fromm, D.P., Kino, G.S., Moerner, W.E. "Toward nanometer-scale optical photolithography: utilizing the near-field of bowtie optical nanoantennas", *Nano Lett.* 6, 355-360 (2006).
- [24] Søndergaard, T., Bozhevolnyi, S., "Slow-plasmon resonant nanostructures: scattering and field enhancements", *Phys. Rev. B* 75, 073402 (2007).
- [25] Crozier, K.B., Sundaramurthy, A., Kino, G.S., Quate, C.F., "Optical antennas: resonators for local field enhancement", *J. Appl. Phys.* 94, 4632-4642 (2003).
- [26] Ebbesen, T.W., Lezec, H.J., Ghaemi, H.F., Thio, T. and Wolff, P. A., "Extraordinary optical transmission through subwavelength hole arrays", *Nature* 391, 667-669 (1998).
- [27] Bravo-Abad, J., Martin-Moreno, L. and Garcia-Vidal, F.J., "Transmission properties of a single metallic slit: from the subwavelength regime to the geometrical optical limit", *Phys. Rev. E* 69, 026601 (2004).
- [28] Gordon, R. "Light in a subwavelength slit in metal: propagation and reflection", *Phys. Rev. B* 73, 153405 (2006).
- [29] Xie, Y., Zakharian, A.R., Moloney, J.V. and Mansuripur, M., "Transmission of light through slit apertures in metallic films", *Opt. Express* 12, 6106 (2004).
- [30] Vincenti, M. A., Petruzzelli, V., D'Orazio, A., Prudeniano, F., Bloemer, M. J., Akozbek, N. and Scalora, M., "Second harmonic generation from nanoslits in metal substrates: applications to palladium-based H₂ sensor", *Journal of Nanophotonics* 2, 021851 (2008).
- [31] Vincenti, M. A., De Sario, M., Petruzzelli, V., D'Orazio, A., Prudeniano, F., de Ceglia, D., Akozbek, N., Bloemer, M.J., Ashley, P. and Scalora M., "Enhanced transmission and second harmonic generation from subwavelength slits on metal substrates", *Proceedings of SPIE* 6987, 69870O (2008).
- [32] Romero, I., Aizpurua, J., Bryant, G.W., Garcia de Abajo, F.J., "Plasmons in nearly touching metallic nanoparticles: singular response in the limit of touching dimers", *Optics Express* 14, 9988-9999 (2006).
- [33] Bakker, R.M., Boltasseva, A., Liu, Z. Pedersen, R.H., Gresillon, S., Kildishev, A.V., Drachev, V.P. and Shalaev, V.M. "Near-field excitation of nanoantenna resonance", *Optics Express*, 15, 13682- 8, (2007).
- [34] Smythe, E. J., Cubukcu, E. and Capasso, F., "Optical properties of surface plasmon resonances of coupled metallic nanorods" *Optics Express* 15, 7439- 47 (2007).
- [35] Marrocco, V., Vincenti, M. A., Mongiello, A., De Sario, M., Petruzzelli, V., Prudeniano, F. and D'Orazio, A. "Gold nanorods in linearly modulated array", *Proc. Metamaterials 2009, 3rd International Congress on Advanced Electromagnetic Materials in Microwaves and Optics, London (UK) August 30th -September 4th* (2009).
- [36] Palik, E. D., [Handbook of Optical Constants of Solids], Academic New York, 1985.